Final Draft
of the original manuscript:

Nasermoaddeli, M.H.; Lemmen, C.; Stigge, G.; Kerimoglu, O.; Burchard, H.; Klingbeil, K.; Hofmeister, R.; Kreus, M.; Wirtz, K.W.; Koesters, F.:

A model study on the large-scale effect of macrofauna on the suspended sediment concentration in a shallow shelf sea

In: Estuarine, Coastal and Shelf Science (2017) Elsevier

DOI: 10.1016/j.ecss.2017.11.002

Large-scale effect of macrofauna on suspended sediment concentration in a shallow shelf sea (southern North Sea)

Nasermoaddeli, M. H.[a], Lemmen, C.[b], Kösters, F.[a], Stigge, G.[c], Kerimoglu, O.[b], Burchard, H.[d], Klingbeil, K.[d], Hofmeister, R.[b], Wirtz, K. W.[b]

[a] Federal Waterways Engineering and Research Institute (BAW), Hamburg, Germany

[b] Helmholtz-Zentrum Geesthacht Zentrum für Material- und Küstenforschung, Institute of Coastal Research, Geesthacht, Germany

[c] Institute for Applied Ecology (IfAÖ GmbH), Rostock, Germany

[d] Leibniz Institute for Baltic Sea Research Warnemünde, Dept. for Physical Oceanography and Instrumentation, Rostock, Germany

Abstract

Biological activities of macrofauna on the sea floor mediate suspended sediment dynamics, at least locally. Most previous studies and modeling efforts were directed towards the local and small-scale effects of macrofauna on suspended sediment dynamics, and abundance estimates relied on rough assumptions. In the present work, the large-scale biological contribution of macrofauna to sediment dynamics (exemplified by a bivalve, the bean-like *Fabulina fabula*, formerly known as *Tellina fabula*) based on its observed distribution in the southern North Sea is investigated. Macrofauna effects have been considered with respect to the critical bed shear stress and erodibility, which are two important factors that control the resuspension rate. Simulation results for a typical winter month revealed for the first time that the suspended sediment concentration (SSC) is increased not only locally but beyond the inhabited zones. This effect is not limited to the near-bed water layers but can be observed throughout the entire water column, especially during storm events. We show that the magnitude of changes in SSC due to macrofauna effects depends not only on macrofauna abundance, but also on sediment transport parameters and hydrodynamic conditions as well as on sediment availability. For a selected storm event in February 2010, we succeeded to explain the counter-intuitive decrease of near-bed SSC in areas with large macrofauna abundance compared to a simulation excluding this macrofauna: A high macrofauna-induced entrainment rate leads to quick exhaustion of the available sediment at the bed and consequently limits the near-bed SSC. We also

find that for the southern North Sea a single characteristic suspended sediment fraction may sufficiently describe biologically influenced suspended sediment dynamics.

Key words: macrofauna, biological effect, suspended sediment, North Sea, Fabulina fabula, numerical modelling

1 Introduction

Suspended sediment dynamics in coastal and shelf seas critically affects major biological processes and has significant economic implications (Puls *et al.,* 1997, Winterwerp and van Kesteren 2004, Gayer *et al.,* 2006, van der Molen *et al.,* 2009). The transport of suspended sediment makes an important contribution to material fluxes between the sea bed and the water column and between rivers, shallow water systems, and the open sea. Transport of suspended sediment depends on physical factors such as tides and their asymmetry (Burchard *et al.*, 2008; Gräwe *et al.*, 2016), wind and wave forcing (Lettmann *et al.*, 2009), and morphological characteristics of the seafloor (van Ledden *et al.*, 2004). Sediment transport is, however, increasingly believed to also be affected by biological factors such as the coverage of the seafloor by microphytobenthos and macrofauna (Rhoads *et al.,* 1978, Jumars and Nowell, 1984, Krumbein, 1994, Paterson*,* 1997, Widdows et al., 1998, Deckere *et al.,* 2001, Orvain *et al.,* 2006, Montague*,* 2013, Briggs *et al.,* 2015, Harris *et al.,* 2016). Benthic organisms exert a significant influence on sediment dynamics (3-6 times increase of re-suspension rate as reported by Davis (1993)), since their activity is linked to a large number of biological, geological, and physical factors. For example, macrobenthic animals graze on stabilizing microphytobenthos (Orvain *et al.,* 2014), change the roughness of the seafloor (Peine *et al.,* 2005), or directly release particles into the water column (Graf and Rosenberg*,* 1997).

In this study we focus on two macrobenthic modifications of suspended sediment dynamics: changes in (1) the critical bed shear stress for erosion and (2) the erodibility of the bed sediment. These two parameters, together with actual bottom shear stress, strongly determine erosion and resuspension rates (Pleskachevsky *et al*., 2005 Stanev *et al*., 2009) and have been identified as sensitive parameters in previous modeling studies (Knaapen *et al.,* 2003, Lumborg *et al.,* 2006, Le Hir *et al.,* 2007, Sanford*,* 2008, Borsje *et al.,* 2008, van Prooijen, Bram C. *et al.,* 2011, Orvain *et al.,* 2012).

Sediment erodibility of the few upper centimeters of the bed layer is modified (van Hulten *et al.,* 2014; Armanini and Di Silvio*,* 1986), for example, by moving, sheltering and feeding macrofauna.

These highly seasonal processes lead to sediment displacement and are subsumed under the term bioturbation (Le Hir *et al*., 2007). They also alter sediment aggregation (Nowell and Jumars, 1984), porosity and permeability (Graf, Rosenberg, 1997), and the erodibility of the bed layer through biostratification. For example, the active and diffusive vertical transport by upward conveyors (e.g. tube building lugworm *Arenicola marina*) increases the fine fraction at the water--sediment interface. Conversely, downward conveyors (e.g. sipunculid worms) decrease the fine fraction (Wheatcroft and Butman, 1997).

Burrowing and grazing activities of the deposit feeder *Fabulina fabula* (*F. fabula*) formerly known as *Tellina fabula*, for example, increases the erodibility of surface sediments (Austen *et al.*, 1999). Sediment erodibility can be further altered by aggregation of bulk sediment into fecal pellets or pseudo-feces by deposit feeders. This bio-aggregation increases erodibility, since the aggregated material is less cohesive than before consumption (Austen *et al.*, 1999). Fecal pellets are also more prone to erosion due to the reduction of specific surface area, i.e. the ratio of surface area to mass (Andersen and Pejrup, 2011).

Critical bed shear stress of the uppermost bed layer is also reduced by the generation of a fluff layer, which may form by tracks of snails, fecal pellets and disintegrated sediment particles due to deposit feeding activities (Orvain *et al.*, 2003). Particles from this layer are brought into suspension far below the critical bed shear stress of the underlying sediment ("fluff layer erosion") (Shimeta *et al.*, 2002).

Research on suspended sediment dynamics has started to include macrobenthic effects, specifically on erodibility, in both observational and modeling studies. Most of these past studies, however, focused on local effects of benthic fauna (benthos) on sediment transport or were restricted to smaller, e.g. intertidal scales (Paarlberg *et al.*, 2005; Borsje *et al.,* 2007; Le Hir *et al.,* 2007; Sanford, 2008). Large-scale effects of benthic fauna on suspended sediment dynamics have been scarcely studied so far (e. g. in Seifert *et al.* (2009) for the Baltic Sea).

Here, we quantify local effects and study how these impact the large-scale distribution of suspended sediments. The present study particularly aims to answer the following questions: (1) To what extent and magnitude do macrobenthic effects on critical bed shear stress and erodibility influence the large-scale near-bed suspended sediment distribution in a shallow shelf-sea (southern North Sea)? (2) Are the effects similar for different sediment classes? (3) Do effects differ for

sediment transport near the bed and in the whole water column? (4) Are the biological impacts event-driven or characteristic for longer time periods?

We address these questions by devising a coupled model system that resolves the relevant processes for coastal sediment transport. This coupled system includes effects of macrofauna by using the observed spatial distribution of bivalve *F. fabula, which* is a dominant species and eponymous characteristic of a macrozoobenthos community of the southern North Sea. We then compare simulated surface suspended sediment concentration (SSC) with satellite observations and in situ measurements and analyze the simulation results for a reference scenario including all processes and another scenario that disregards the macrobenthic effects.

2 Materials and methods

2.1 Study Area

The study area comprises the southern North Sea, a shallow coastal system with water depths of up to 50 m, intertidal flats and a number of estuaries at the coastline (Figure 1). Currents are dominantly influenced by the semi-diurnal tides which propagate through the German Bight in an anti-clockwise sense, with amplifications in the estuaries and complex bathymetric interactions (Stanev *et al.*, 2014). Substantial quarter-diurnal tidal components are generated (Stanev *et al.*, 2014), which show a significant seasonal signal (Gräwe *et al*., 2016). The tidal range varies from 2 m near the Dutch coast to about 4 m in the German estuaries. Tidal mixing inhibits thermal and haline stratification in the shallower parts of the German Bight (Schrum, 1997). Coastal upwelling and downwelling due to wind forcing affect the pathways of the discharge from the Elbe, Weser and Ems rivers (Krause *et al.*, 1986). Stratification only occurs seasonally in the deeper parts of the southern North Sea and occasionally near the estuaries (van Leeuwen *et al.*, 2013). At the fronts between the mixed German Bight waters and the stratified North Sea waters, a so-called line of no return (Postma, 1984) defines an area within which sediments are trapped in the German Bight. Between this line of no return and the coast, a thermohaline overturning circulation transports sediments towards the coast (Burchard and Badewien, 2015), such that sediments are accumulating in the Wadden Sea (Burchard *et al*., 2008) and as estuarine turbidity maxima in the estuaries (e. g. Kappenberg and Grabemann, 2001).

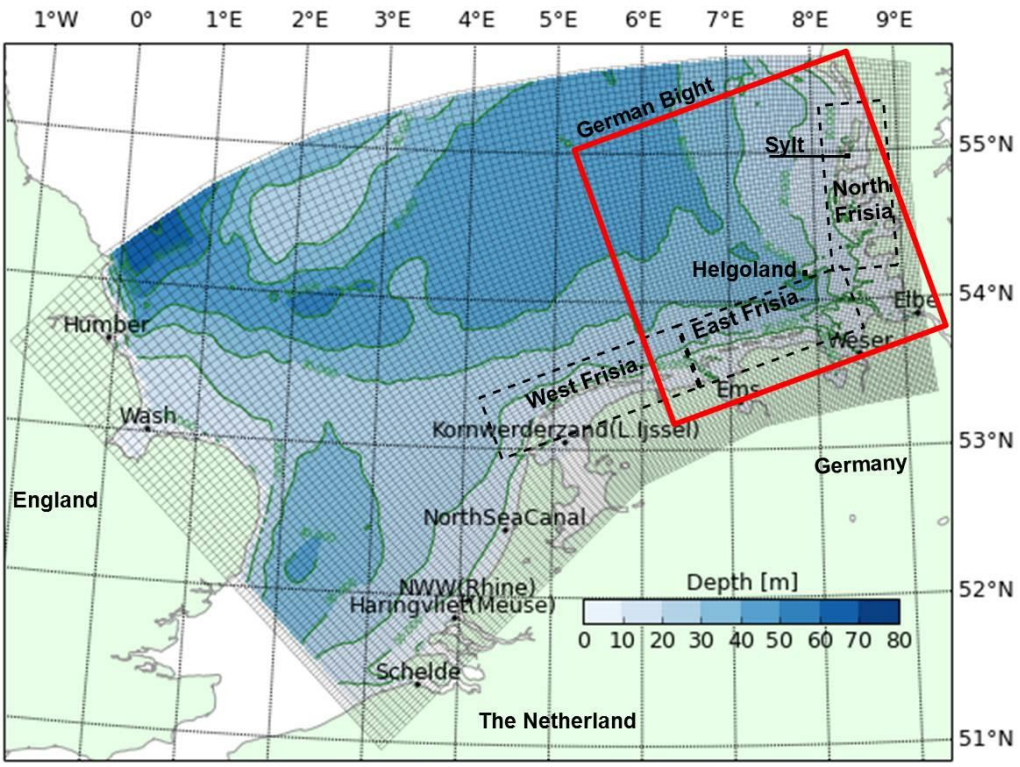

Figure 1 Bathymetry of the southern North Sea as represented on the numerical model grid. The study area of the German Bight is depicted by the red rectangle

Macrobenthic infauna of the German EEZ has been classically categorized into five main benthic infauna communities based on preferred habitat conditions (depth, sediment type), namely, *Amphiura filifornis, Tellina (Fabulina) fabula, Nucula nitidosa, Goniadella-Spisula, Spio filicornis (*Salzwedel *et al., 1985)*. The categorization has been roughly confirmed by the ICES North Sea Benthos Survey (Duineveld *et al.*, 1991) and the North Sea Benthos Project 2000 (Kröncke *et al.*, 2011) using a grid of sampling points, and by more refined cluster analysis (Neumann *et al.*, 2012)

2.2 Observational data

2.2.1 Macrofauna data

In the present study we accessed the macrozoobenthos database of the Institute for Applied Ecology (IfAÖ GmbH) which included 17710 hauls at 2347 infauna sampling stations and 2798 hauls at 1049 epifauna sampling stations in the German Bight by the time of query. Based on an analysis of species abundances, biomasses and presences derived from this database and by means of a specialist literature review, certain species were chosen that are particularly important for sediment

transport processes. Due to its bioturbation potential the bivalve *F. fabula* is among the most distinctive species of the study area (Borsje *et al.*, 2009) which is also reflected by the naming of the *F. fabula* community that occurs in the German Bight (Rachor and Nehmer, 2003). The distribution of *F. fabula* in the southern North Sea was compiled based on observations in the German EEZ (Dannheim, 2014), which were extrapolated using available data (Creutzberg, 1986, Reiss *et al.*, 2011 ; van Moorsel, 2011 ; Dannheim, 2014) to the entire study area as shown in Figure 2.

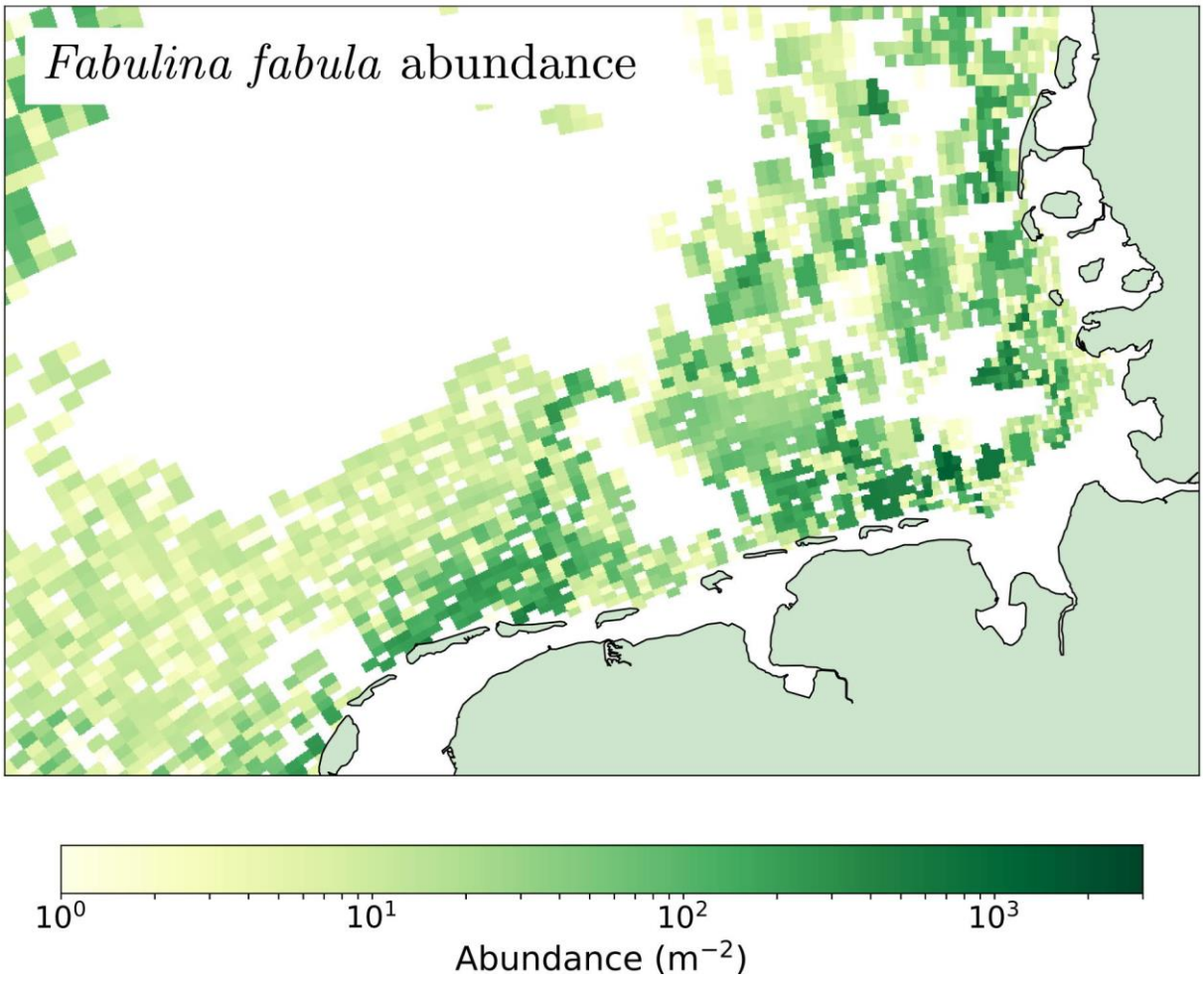

Figure 2 Interpolated annual mean abundance of the bivalve *F. fabula* in the southern North Sea Station data (Individuals m^{-2})

Near-surface in situ time series in the area of West Frisia provided by the Dutch authority Rijkswaterstaat was accessed through OpenEarth (Rijkswaterstaat, 2017). The data covers measurement locations along cross-shore transects at low temporal resolution. The two stations

Terschelling and Rottumerplate (see Figure 3) were selected because of their close proximity to the East Anglia plume and data availability for the period of study.

2.2.2 Satellite data

Suspended sediment concentrations close to the water surface can be inferred from Envisat satellite images provided by the European Space Agency (ESA) at 300 m resolution. The satellite images were pre- and post-processed by ESA and Brockmann Consult using MERIS regional case 2 water algorithms (C2R) explained in Doerffer *et al.* (2006). It should be noted that the calculated concentrations represent the total suspended matter of the near-surface layers, which also includes organic matter that is not considered in the simulated SSC. The penetration depth of the light emitted from the satellite-borne MERIS sensor depends on the turbidity of the water, for example 1 m deep in case of high turbidity in our area of interest.

2.3 Numerical models

To investigate large-scale macrofauna effects on the suspended sediment transport in the southern North Sea, a generic benthos module (Nasermoaddeli *et al.*, 2014) was coupled to hydrodynamics, sediment transport, and erosion—sedimentation models via the Modular System for Shelves and Coasts (MOSSCO, Lemmen *et al.*, 2013; Hofmeister *et al.*, 2014; Lemmen *et al.*, 2017) coupling framework. The MOSSCO framework is built on and extends the Earth System Modeling Framework (ESMF, Hill *et al*., 2004)

Apart from five model components (hydrodynamics, suspended sediment, erosion—sedimentation, waves and benthos effect) MOSSCO entails a generic input components that provide data on ocean boundary particle concentration, river loads and macrofauna distribution.

2.3.1 Hydrodynamic model

Hydrodynamics is simulated by the General Estuarine Transport Model (GETM; Burchard and Bolding, 2002). GETM is an open source coastal ocean model, which has been proven high skill in various studies for the North Sea and Wadden Sea (Stips *et al.*, 2004; Burchard *et al.*, 2008; Lettmann *et al.*, 2009; van Leeuwen *et al.*, 2013; Duran-Matute *et al.*, 2014; Purkiani *et al.*, 2016, Gräwe *et al.*, 2016). It solves the incompressible Navier-Stokes-Equations and additional prognostic

equations for temperature and salinity (Klingbeil and Burchard, 2013). The free surface is calculated efficiently in an explicit mode-splitting algorithm and supports drying-and-flooding of intertidal flats. Quantities are transported with high-order, directional split TVD-schemes, which minimize numerical mixing (Klingbeil *et al.*, 2014; Mohammadi-Aragh *et al.*, 2015). Horizontal sub-grid scale dynamics are parametrized by a Smagorinsky closure (Smagorinsky, 1963). Turbulent vertical viscosities and diffusivities are provided by the General Ocean Turbulence Model (GOTM) which offers state of the art turbulence closure from Umlauf and Burchard (2005). For the present study a dynamic k-ε model with the 2nd-order closure of Canuto *et al.* (2001) "Model A" was applied. Bottom stresses are calculated based on the law of the wall with a prescribed bottom roughness length (here z_0=1 mm). These current-only bottom stresses are modified according to Soulsby (1997) and consider the combined wave—current stresses. Significant wave height and wave peak period were parametrized in terms of local depth and wind conditions (Breugem and Holthuijsen, 2007).

2.3.2 Sediment transport model

Suspended sediment is here represented by three size classes. Sediment mass is transported along the current vector computed by the hydrodynamic model, while diffusion due to turbulence and downward movement with a constant, size-dependent sinking velocity are applied additionally in the vertical. For the transport of the SSC, the same high-order, directional split TVD-schemes are used as for the transport of salinity and temperature in the hydrodynamic model. At open sea and river boundaries constant sediment concentration is prescribed as proposed by Gayer *et al.* (2006). At water-sediment interface, the net mass flux for each suspended sediment size class is prescribed as flux boundary condition for the sediment transport model.

The modularity within MOSSCO allows the coupling of a separate model for the calculation of the net sediment flux at the water—sediment interface. For this purpose, the erosion—sedimentation routines of the Deltares Delft3d model were encapsulated and coupled via an ESMF interface to MOSSCO (Nasermoaddeli *et al.*, 2014). The model uses the well-known Partheniades-Krone equation (Partheniades, 1965) for calculating the net sediment flux of cohesive sediment at the water—sediment interface (see Table 1).

Table 1: Erosion and deposition fluxes as implemented in the numerical model following Partheniades (1965)

$E^l = g \cdot M^l \cdot S(\tau, \tau_{cr,er}^l)$	Eq. 1
$D^l = w_s^l \cdot c_b^l \cdot S(\tau, \tau_{cr,dep}^l)$	Eq. 2
$S(\tau, \tau_{cr,er}^l) = \begin{cases} \left(\frac{\tau}{f \cdot \tau_{cr,er}^l} - 1\right), & \tau > \tau_{cr,er}^l \\ 0, & \tau \leq \tau_{cr,er}^l \end{cases}$	Eq. 3
$S(\tau, \tau_{cr,dep}^l) = \begin{cases} \left(1 - \frac{\tau}{\tau_{cr,dep}^l}\right), & \tau < \tau_{cr,dep}^l \\ 0, & \tau \geq \tau_{cr,dep}^l \end{cases}$	Eq. 4

The main parameters taken into account are erosion flux E (kg m^{-2} s^{-1}) and the deposition flux D (kg m^{-2} s^{-1}). l is the index of sediment class, g the biological destabilization factor for erodibility (Eq. 6), M the erodibility factor (kg m^{-2} s^{-1}), S the Heavy-Side function, w_s the settling velocity for each sediment class l, c_b the near bed suspended sediment concentration, τ the bed shear stress, $\tau_{cr,er}$ the critical bed shear stress for erosion, f the biological destabilization factor for critical bed shear stress for erosion, and $\tau_{cr,depr}$ the critical bed shear stress for deposition. The factors f and g introduced here to the original formula are to account for macrofauna effects presented in the following section.

The net vertical sediment flux for each class results from the difference between erosion and deposition, both of which are applied to the active single layer of the bed. In this approach, the bed is conceptualized as a well-mixed non-stratified layer with a given depth. An arbitrary number of sediment size classes can be considered within this highly idealized sediment inventory. The mass fraction of each sediment size class within the well-mixed layer is the ratio of its mass to the total mass of all fractions within the layer. The mass of each sediment size class for a unit area is initialized in the model by a given fraction, thickness, porosity and sediment dry density which is spatially constant. The deposited mass of each sediment size class is added to the rest of the mass of the same class within the layer and mixed instantaneously with the bed material throughout the whole layer thickness. Hereby, the mass fraction of the size class is changed for the whole depth, accordingly. In a similar manner, erosion of bed material for each sediment size class is calculated.

2.3.3 Benthos model

Inclusion of biotic effects on sediment transport modelling is complicated partly by the lack of data and knowledge to quantify effects of biological processes on sediment transport, especially at the community level; further complicacy stems from the seasonal variation of biological components, spatial patchiness, and non-linear interactions within the benthic community (Le Hir *et al.*, 2007). In addition, effects on sediment transport properties are highly specific, thus depend on the function of the considered benthic species, while collective effects of different species on sediments are difficult to predict due to reciprocal (antagonistic) influences in benthic communities (Kristensen *et al.*, 2013).

Currently available models of sediment transport only depict in a very simplified manner the high complexity of effects that macrozoobenthos in their entirety exert on the water-sediment boundary layer. Another issue is the lack of species- or community-specific parameterizations of macrofauna effects on sediment transport parameters. Most sediment transport models which resolve macrozoobenthos were so far parameterized only for few selected macrofauna species and with few affected sediment transport parameters (e.g. Wood and Widdows, 2002; Knaapen *et al.*, 2003; Paarlberg *et al.*, 2005) or they quantify such effects using process-based differential equations (e.g. François *et al.*, 1997; Orvain *et al.*, 2003; Orvain, 2005; Montserrat Trotsenburg, 2011; Orvain *et al.*, 2012).

Due to the lack of suitable parameterizations for *F. fabula*, we applied parameterizations which were originally derived for the effect of *Macoma balthica* on critical bed shears stress and erodibility (Knaapen *et al.*, 2003; Paarlberg *et al.*, 2005).

Our analysis of macrobenthic communities based on the trait-matrix by Darr *et al*. (2014) enabled a generalization of a species specific parametrization. Underlying (laboratory) studies are usually performed suing a single species and now can be extrapolated to specific communities. Given the extremely high number of macrobenthic species in coastal and shelf habitats, we encourage to further develop trait-based approaches, also for keeping model complexity and parametrization effort small.

These two formulations are used as linear modification factors of the corresponding abiotic parameters. It should be noted that both relations rely on only few data collected by Widdows *et al.* (2000a, b) in an intertidal basin. The destabilization factor for critical bed shear stress and erodibility are given in Table 2.

Table 2: Factors accounting for destabilization of critical bed shear stress (f_d) and erodibility (g_d)

$f_{\mathrm{d}}(\mathrm{M}) = 0.0016 \cdot \ln(M^2) - 0.085 \cdot \ln(M) + 1$	Eq. 5
$g_{\mathrm{d}}(M) = \frac{b_2 \cdot \gamma}{(b_2 + \gamma \cdot b_1^M)\, I}$	Eq. 6

f_{d} is the destabilizing factor for critical bed shear stress, *M* is the dimensionless abundance (actual abundance of individuals (ind.) divided by reference abundance of 1 ind. m^{-2}), and g_{d} the destabilizing factor for erodibility. The derivation of Eq. 6 is based on the assumption that the biological effect reaches a maximum with increasing abundance *M*, after which it remains constant (S-shaped curve). The parameters applied here are the maximum biological erosion coefficient $\gamma = 6 \times 10^{-7}$ ms^{-1}, the erosion coefficient without biological influence $I = 4.68 \times 10^{-8}$ ms^{-1} and the regression coefficients $b_1 = 0.995$ and $b_2 = 5.08\ 10^{-8}$ ms^{-1}.

The mentioned parameterizations were implemented in MOSSCO's benthos module, which is a generic object-oriented library. It provides an adaptive structure for linear superposition of macrofauna effects on sediment transport parameters such as critical shear stress, erodibility, roughness, settling velocity, biodeposition and bio-resuspension.

2.4 Model setup

The model resolves three silt classes , which differ in settling velocity and transport parameters, similar to Gayer *et al*. (2006) and compliant to measurements of Puls *et al.* (1995) in the German Bight. Other sediment transport parameters for each silt class are presented in **Fehler! Verweisquelle konnte nicht gefunden werden.**3.

The initial fraction of each silt class at the bed and in the water column was assumed spatially constant in the computational domain. They were determined by multiplying measured silt fractions in the shallow water (0-20 m) zone by the ratio of the area of shallow zone to the total area of the southern North Sea. The silt fractions at open sea boundaries and rivers were selected according to Gayer *et al*. (2006).

The initial thickness of the active layer was chosen to be 10 mm to limit the available initial sediment at bed, which is not very far from values (2-5 mm) obtained by Lumborg *et al.* (2006) based

on field observations for the upper bed layer in Kongsmark, a tidal mudflat in the Danish Wadden Sea.

The critical bed shear stress for erosion ($\tau_{c,er}$) of very fine silt was calculated according to the thresholds of bottom shear stress velocity for benthic fluff mud blanket and coarse silt given in Gayer *et al.* (2006). The critical bed shear stress of 0.6 N m^{-2} for fine silt was calibrated by comparing the simulated SSC with available satellite data and in-situ measurements.

The existence of a critical bed shear stress for deposition ($\tau_{c,dep}$) is under debate. Winterwerp (2007) showed the irrelevance of $\tau_{c,dep}$ by reproducing successfully experimental results without inclusion of this parameter in his model. In contrast, Maa *et al.* (2008) argue that deposition ceases beyond a specific bed shear stress based on their laboratory experiments. We carried out a sensitivity analysis by testing a range of values of $\tau_{c,dep}$ for each silt class varying between 0.096 N m^{-2} to 2 N m^{-2}, as well as ignoring this parameter. The selected range reflects literature values (i.e. Gayer *et al.*, 2006, and Lumborg *et al.*, 2006). The best fit between simulated and measured SSC was reached by the values of $\tau_{c,dep}$ given in **Fehler! Verweisquelle konnte nicht gefunden werden.**3. Also erodibility, constant for the three silt fractions, was calibrated.

Table 3: Sediment parameters in of the numerical model (SNS setup)

Silt class	Settling velocity (m s^{-1})	Initial Fraction* (%)	Initial concentration (g m^{-3})	Initial thickness (m)	$\tau_{c,er}$ (N m^{-2})	$\tau_{c,dep}$ (N m^{-2})	Erodibility (kg m^{-2} s^{-1})
coarse	0.001	8.24	2.5	0.01	0.78	-	1.0×10^{-5}
fine	0.0001	5.46	2.5	0.01	0.6	1.5	1.0×10^{-5}
Very fine	0.00002	1.21	0.5	0.01	0.1	1.5	1.0×10^{-5}

*fraction in respect to the total mass including all other sediment size classes, for example sand

2.5 Model setup

The model domain covers large parts of the southern North Sea (SNS). We use a curvilinear horizontal grid with 140x100 grid points in the horizontal to align the main axes with the coastline and to increase the resolution in the German Bight up to 1.5 km at the South East corner and 4.5 km at the North West corner (see Figure 1 for the model grid). In the vertical, 20 sigma layers are used, which results in a vertical resolution of 0.5 m in 10 m water depth and 2.0 m in 40 m water depth. This strategy has been shown to work successfully in hindcast simulations with GETM (Hofmeister *et al.*, 2013, Hetzel *et al.*, 2015).

The numerical time step as well as coupling time step among the components was set to 2 minutes. The setup is forced with output data from a regional atmospheric model at the sea surface and the sea surface height at the open boundaries is taken from a barotropic hindcast simulation. A more detailed description of the setup and its validation is given in Kerimoglu *et al.* (in prep.). The effect of bottom friction is implemented as temporally and horizontally constant. The bathymetry of the model domain and model grid is shown in Figure 1. Ten major rivers along the coasts in the southern North Sea were considered with respect to the freshwater fluxes and the suspended sediment loads (Radach and Pätsch, 2007).

Suspended sediment concentration was available only in the Humber and the four rivers which are collectively referred to as the 'Wash' with constant silt concentration (different for each river). For the other rivers, the silt fraction was chosen according to Gayer *et al.* (2006). We prescribe the suspended sediment concentration at the northern and western open boundaries of the model domain using estimates of total SSC by Heath *et al.* (2002).

The simulation period from January to September, 2010 covered both winter as well as summer months (for qualitative assessments) but also matches availability of validation data for hydrodynamic and partly for suspended sediment. For the fully coupled simulation of sediment transport (including macrobenthic effects), the observed distribution of the bivalve *F. fabula* was implemented as modular forcing. The configuration used for this study can be reproduced by downloading the open source MOSSCO setups repository from https://sf.net/p/mossco/setups , selecting the „sns“ example setup with the „spm“ configuration.

3 Results

3.1 Model validation

The hydrodynamic model provides a realistic description of horizontal mixing as inferred from domain-scale salinity gradients and vertical stratification from May to September within the deeper (> ~30 m) regions of the German Bight (Kerimoglu *et al.*, in prep.).

For the SSC validation, two satellite images on March 1, and April 14, 2010 were selected (Figure 3 a, c). The former is representative for a storm event and the latter for a typical neap tide. Both images display the typically observed coastal gradient (strongly decreasing offshore concentration) as well as the East Angelia plume.

Their comparison with simulated near-surface total SSC confirmed a high model skill in terms of reproducing the coastal gradients in the eastern part of the German Bight; but SSC at the Elbe and Weser estuaries are overestimated and at the Ems estuary underestimated, which could be due a too coarse resolution of estuarine dynamics, as addresses by Kerimoglu *et al.* (in prep). The East Angelia plume could be also fairly well reproduced on March 1 (Figure 3 a, b). It is, however, missing in the simulation results on April 14 (Figure 3 c, d). It should be noted that the satellite images show total suspended matter and simulations only suspended sediment concentration.

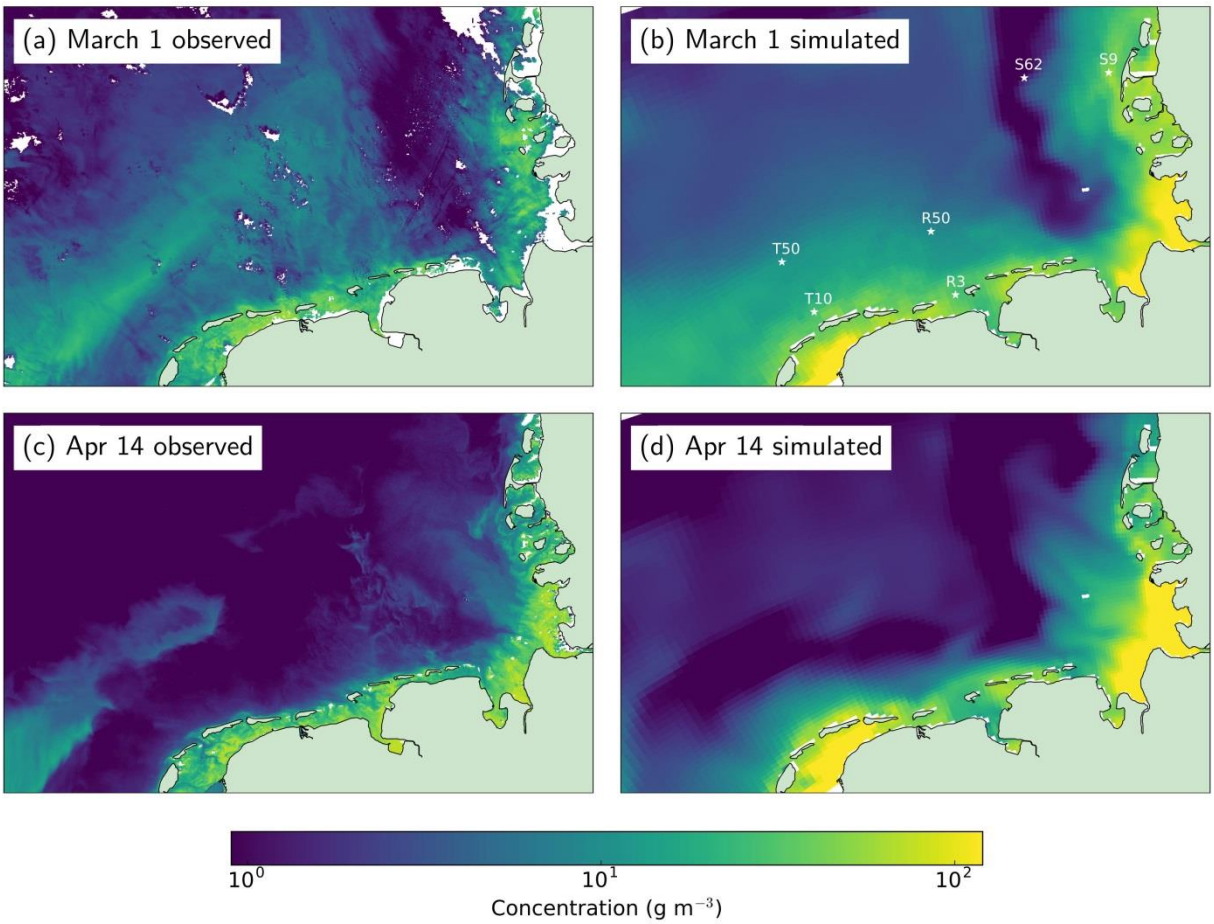

Figure 3 Total suspended matter (TSM) calculated from satellite images on March 1, 2010 (a) and April 14, 2010 (c) vs simulated total suspended sediment concentration (SSC) near-surface at the same days (b and d)

The sediment transport model was further validated using the time series from satellite images as well as in-situ near-surface SSC at several locations nearshore and offshore of West Frisia. Near-surface simulated SSC with and without macrofauna compare relatively well to satellite derived data (Figure 4). At least the order of magnitude of observations and the simulated near-surface SSC agrees in near shore and offshore regions of West and North Frisia. The temporal variation of SSC could be well reproduced in some periods and locations (for example at Terschelling T50 and Rottumerplate R3, Figure 4b, c), but was overestimated at 10 km off Terschelling (T10, Figure 4a). The simulated SSC scenario without macrofauna performed better at T10, which could be due to the overestimation of *F. fabula* abundance by the extrapolation at this location.

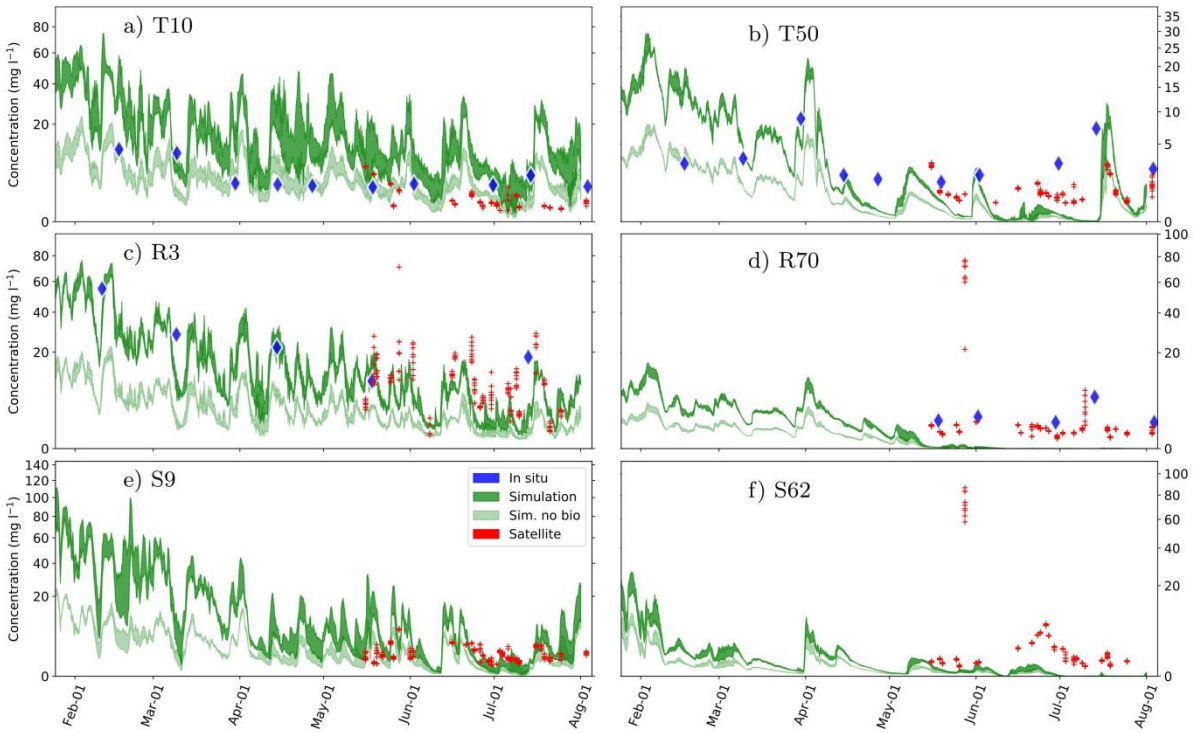

Figure 4 Comparison between in situ measurements (blue diamond), remote sensing observations (red crosses) and simulations (green areas) of concentration of suspended material for coastal transects represented by stations T10 and T50 (10 and 50 km off the Westfrisian island of Terschelling),R3 and R70 (3 and 70 km off the island of Rottumerplate outside the Dollart estuary, and S9 and S62 (9 and 62 km off the Northfrisian island of Sylt); The simulation was sampled in a 2500 m radius around the station and the satellite (with higher resolution than the simulation) in a 500 m radius.

3.2 Simulations with macrofauna effects

In the following the results are presented for a storm event as well as temporal mean effect of macrofauna on SSC. Simulation results for SSC including macrofauna effects (i.e. using the observed spatial distribution of average abundance of *F. fabula*) reveal a number of differences to the scenario without macrofauna.

3.2.1 Storm event

Simulated near-bed SSC with macrofauna effects differs from the SSC in the scenario without macrofauna, depending on the sediment class, macrofauna abundance, and location.

The near-bed SSC of the coarse silt class (Figure 5a) is clumped distributed over a large area in the shallow zone and partly offshore. This patchiness seems to be the imprint of *F. fabula* inhabitation zones, when compared to the contour lines of *F. fabula* abundance in Figure 5b.

Additionally, macrofauna in the model has led not only to an increase of the near-bed SSC in some inhabited areas but also to a decrease in other areas. Zones with reduced near-bed SSC correspond mostly to inhabited zones with higher abundance of *F. fabula* (shown by thicker contour lines). Increases in near-bed SSC due to macrofauna effects were more frequent than reductions and the absolute value of maximum increase (10 g m^{-3}) was larger than the absolute value of maximum decrease (-6 g m^{-3}) as apparent from the histogram in Figure 5a.

Much less patchiness is observed in the near-bed SSC distribution of fine silt class (Figure 5c). A closer comparison of macrofauna enhanced SSC zones with *F. fabula* abundance contours in Figure 5d reveals for the first time (to the knowledge of authors) that near-bed SSC has been modified beyond the zones inhabited by macrofauna modifying sediment erosion and deposition properties. This is particularly obvious in the shallow zones such as north of Sylt or offshore of the Ems estuary, which suggests that biological contribution may trigger large scale modification of near-bed SSC of fine silt. Figure 5d shows a significant macrofauna-related increase of SSC primarily in front of Sylt and also in some parts of the shallow waters along East and West Frisia. These zones correspond to the inhabited regions with *F. fabula* (shown by contour lines).

Also near-bed SSC of fine silt is reduced by macrofauna in a number of regions (Figure 5d). The pattern of near-bed SSC of fine and coarse silt is similar, with the former showing higher magnitudes of change and over larger areas. The near-bed SSC of fine silt has been reduced significantly offshore of West Frisia and along the Elbe glacial channel beyond Helgoland, whereas it has mostly increased for coarse silt due to macrofauna. Similar deviations are noticed to the west and north of Sylt as well as offshore of East Frisia. Seaward of West Frisia, however, macrofauna activities have resulted in a decrease of near-bed SSC of fine silt and coarse silt. Finally, the histogram shows a significant increase of differences due to macrofauna effects (from -15 to 30 g m^{-3}). Here again the number of elements with enhanced SSC due to macrofauna exceeds the ones displaying the opposite trend.

No patchiness can be detected from near-bed SSC distribution for very fine silt in Figure 5e. The modified near-bed SSC due to macrofauna for very fine silt, depicted in Figure 5f, shows a very low difference (almost negligible) and mostly a reduced concentration in coastal shallow areas, irrespective of the *F. fabula* distribution. It is inferred that the macrofauna effect plays no significant role for near-bed SSC for very fine silt during a storm event, in contrast to the other two silt classes.

The concentration of near-bed total silt (sum of all three silt classes) shown in Figure 5g represents similar gradients and magnitude to those of the fine silt fraction. Patchiness of the near-bed SSC offshore along the coasts and the SSC plume west and south west of Helgoland can be still observed. The macrofauna contribution to the near-bed SSC (Figure 5h) is quite similar for near-bed total silt and fine silt class. This implies that the dominant macrofauna effects on the near-bed SSC may be represented by fine silt fractions in case of a storm event. It should be however noted that the magnitude of enhancement of near-bed SSC due to macrofauna decreases when integrating over all silt fractions, since in some regions concentration increased for fine silt, but decreased for coarse silt, such as west of Sylt.

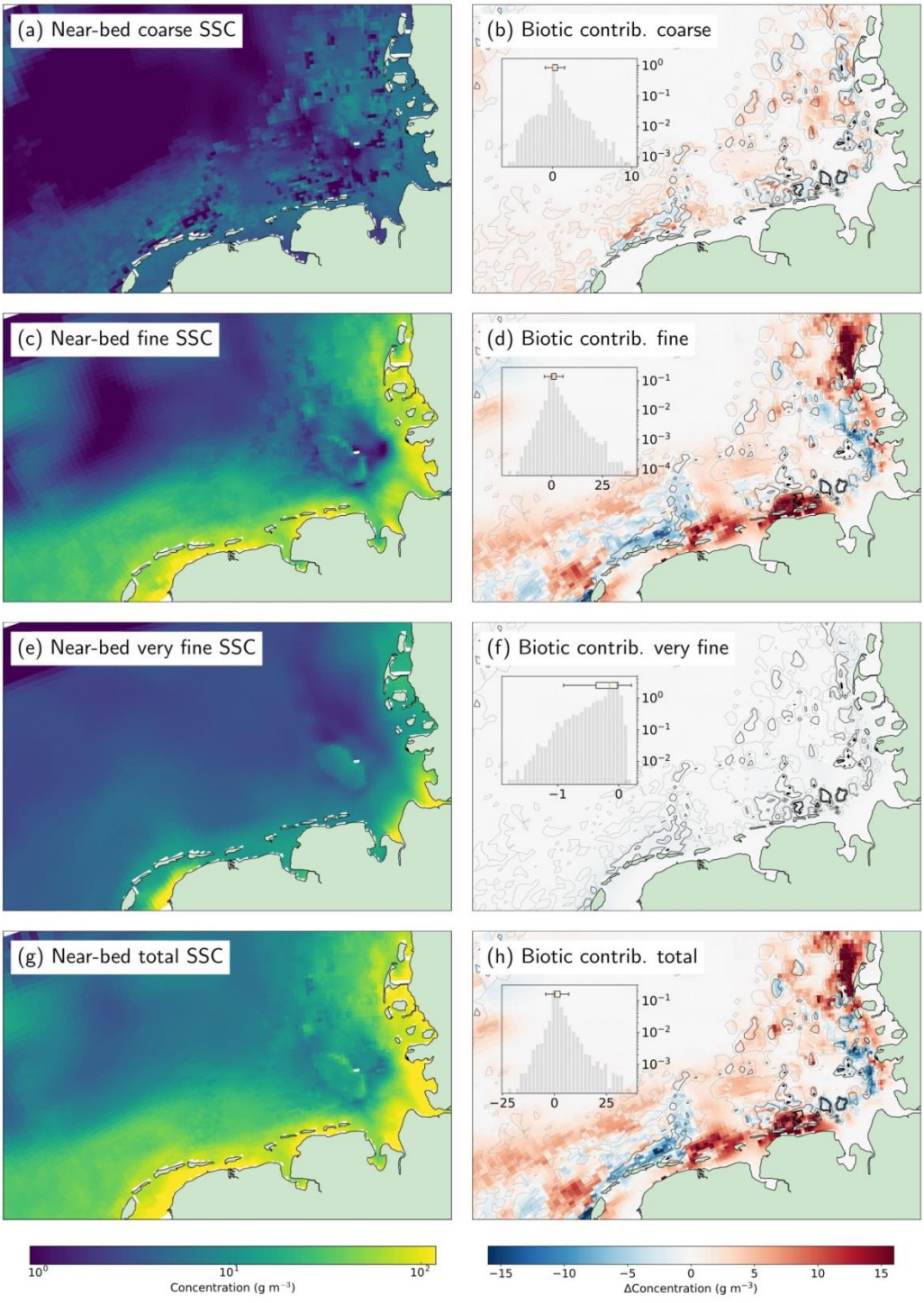

Figure 5 Simulated near-bed suspended sediment concentration (SSC) at a storm event in February 2010. The left hand panels show the near-bed SSC for coarse (a), fine (b), very fine (e) and total (g) SSC; the right hand panels (b, d, f, h) show the calculated modification due to benthos effects, respectively. Contours denote the presence of *F. fabula* at 10, 100, and 500 individuals m^{-2} levels. The histogram shows the logarithmically scaled distribution of biotic modifications in n = 8,997 grid cells.

3.2.2 Depth-averaged SSC

Depth-averaged SSC is especially important for both ecosystem modelling and sediment management and therefore was subject to further investigations. As results for all three silt classes were quite similar to those for near-bed SSC, we present only the total depth-averaged SSC in the following.

The total depth-averaged SSC in Figure 6 shows similar patterns as the total near-bed SSC, except for a weaker patchiness, which is an implication of vertical and horizontal mixing of SSC. The major difference seems to be the plume around Helgoland, which lacks for total depth-averaged SSC and thus appears specific to the near-bed layer. The plume may hence be due to local resuspension of silt near the bed, usually deposited south east of Helgoland (Puls *et al.*, 1999). The horizontal distribution of macrofauna contribution to the depth-averaged SSC shown in Figure 6b is similar to that of near-bed SSC depicted in Figure 5h. This is a significant outcome confirming that biological activities of macrofauna at the sea floor may impact the concentration beyond the extent of the inhabitation zone and throughout the water column, at least in a storm event.

Areas and magnitude of enhanced and reduced concentration due to the macrofauna effects are quite similar for near-bed and depth-averaged values.

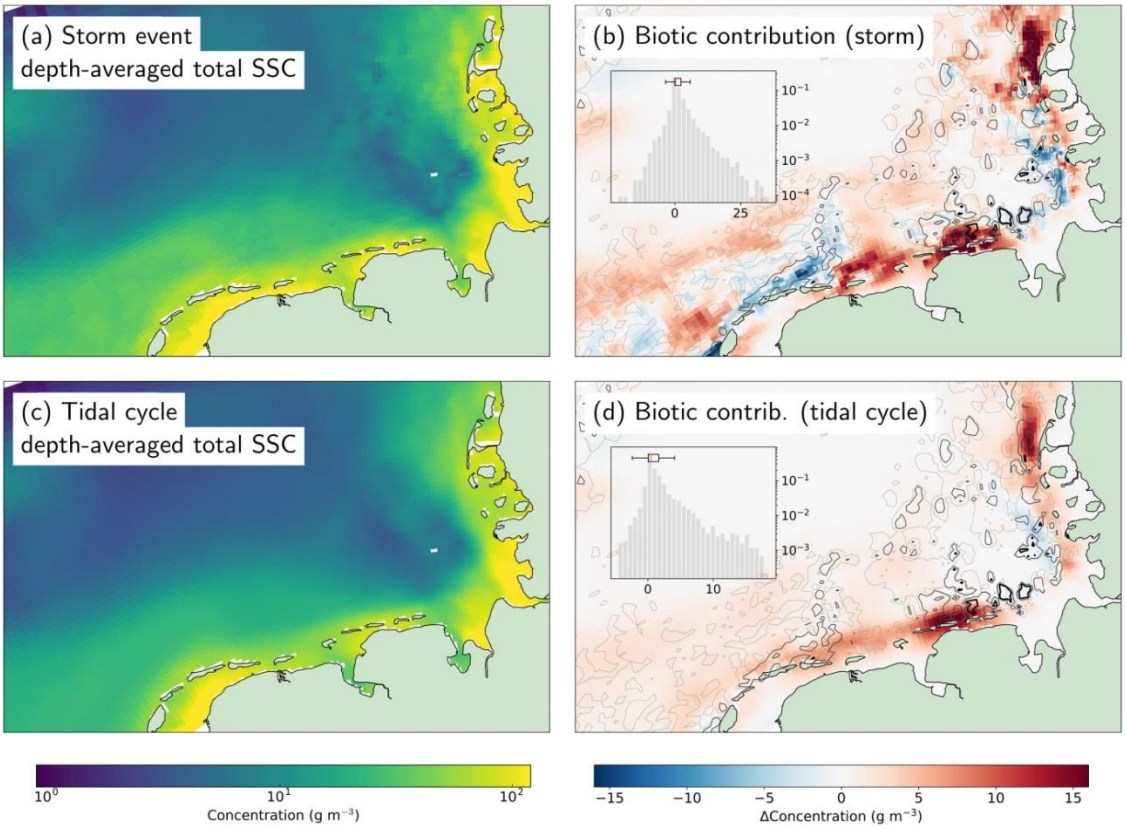

Figure 6 Simulated depth averaged total suspended sediment concentration (SSC) at a storm event in February 2010 (upper panels a,b) and temporally averaged over a tidal cycle in February 2010 (lower panels c,d) . The left hand panels (a,c) show concentration; the right hand panels (b,d) show the included contribution of biotic benthic modification. Contours denote the presence of *F. fabula* at 10, 100, and 500 individuals m^{-2} levels. The histogram shows the distribution of biotic modifications in n = 5,869 grid cells.

3.2.3 Temporal mean macrofauna effects

For a spring-neap tidal cycle during a typical winter month (February 2010), the patchiness of total mean depth-averaged SSC disappears (Figure 6c), in contrast to the storm event (Figure 6a). This may indicate strong horizontal mixing of macrofauna-induced changes in SSC during a spring-neap tidal cycle. It can be furthermore inferred from Figure 6d that mean depth-averaged SSC is generally enhanced by macrofauna in most areas of the southern North Sea, also in contrast to the storm event. Specifically, contrary to the storm event, the SSC is increased offshore of West Frisia due to biological contribution. The only area with slightly decreased SSC is along the glacial valley of the Elbe. The SSC has been biologically increased mostly along the coastal belt and the effect is highest around the East Frisian Islands and Sylt. The magnitude of increased SSC due to the

macrofauna effects is still significant (up to 15 g m^{-3}), but the maximum reduction of SSC reaches to only -3 g m^{-3}.

These results confirm that macrofauna exerts an effect on the spatio-temporal distribution of SSC beyond the inhabited areas and thus invokes a large-scale impact on SSC in the southern North Sea regardless of the physical condition.

4 Discussion

Suspended sediment concentration increases due to macrofauna effects (Davis, 1993, Le Hir *et al.,* 2007) beyond the inhabitation zones for the fine silt class while not so for the coarse silt (Figure 5). This can be explained by the smaller settling velocity of this sediment class (0.0001 m s^{-1}) compared to that of coarse silt, allowing transportation beyond their origin of production . For example, for a residual tidal velocity (root mean square) of 0.2 m s^{-1} and a water depth of 10 m in shallow area, the fine silt can be transported 20 km. Moreover, the biological contribution to fine silt (maximum 30 g m^{-3}) is three times larger than that for coarse silt (histograms in Figure 5b and Figure 5d), which provides more suspended sediment to be transported much farther, triggering a large-scale impact on SSC. The very fine silt at the bed was rapidly exhausted due to its very low critical bed shear stress (0.1 N m^{-2}), making this class of sediment less sensitive to the biologically mediated sediment properties at the bed (erodibility, critical bed shear stress). Therefore, the difference in near-bed SSC between biologically mediated sediment and without biological effect is small. Moreover, the very low settling velocity of particles (0.0002 m s^{-1}) allowed a large spatial distribution of the slightly modified near-bed SSC by horizontal transport processes beyond the inhabited zones.

The unexpected decrease of near-bed SSC in some areas especially those with high abundance (>100 ind. m^{-2}) can be attributed to two factors, biologically mediated entrainment rate and sediment availability (Stammermann and Piasecki, 2012). In model areas covered or dominated by *F. fabula* the erodibility is increased and the critical bed shear stress is decreased. These two processes lead to higher and more frequent resuspension primarily over these zones. Consequently, the mass in bed is eroded more frequently and finally exhausted more quickly than is the case without considering macrofauna-related effects. Figure 7 demonstrates this situation for west of Sylt before and after the storm event. Sediment mass at the bed for the coarse silt had been already exhausted prior to the storm event on February 3 (shown with a vertical green line) so that no

sufficient sediment was available for erosion during the storm (Figure 7b). Compared to the case without macrofauna effects, the sediment mass is at least two orders of magnitude larger and the erosion process is not limited by sediment availability. Consequently, the concentration of near-bed SSC during the storm event is larger for the case without biological effect (light shaded area in the upper Figure 7b).

It was found in Figure 5d that at the same location (west of Sylt) macrofauna resulted in enhancement of the near-bed SSC of fine silt in contrast to a reduction for near-bed SSC of coarse silt. The reason can be demonstrated by sediment availability for both cases (with and without macrofauna effects) presented in Figure 7a. These two figures indicate the importance of sediment availability as a limiting factor for macrofauna effects. Moreover, it can be observed in Figure 7a that the sediment mass is reduced more rapidly, when including macrofauna effects on sediment erodibility and critical bed shear stress (compare the slope of the two curves of the lower diagram just before the storm event).

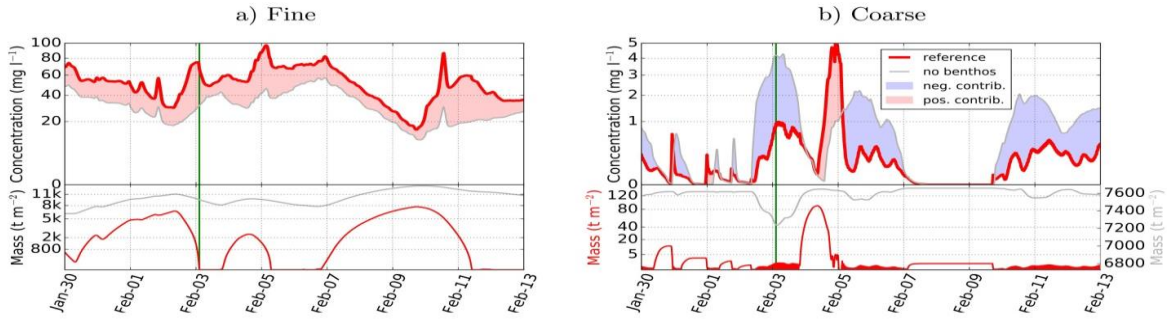

Figure 7 Near-bed simulated suspended sediment concentration (SSC, for coarse and fine silt fractions) including the contribution of biotic modification (blue and yellow shading, upper panel) in the first two weeks of February 2010. Available mass is shown in the lower panel indicating frequent depletion of available sediment for resuspension, especially after the storm event (green line).

Our results have important implications for ecosystem modeling. Light penetration through the water column is affected by increased turbidity induced by macrofauna at the sea bed, which impacts primary production and population dynamics of phytoplankton. This finding indicates the indirect coupling between macrofauna and phytoplankton through SSC. It should, however, be investigated whether such linkage is limited to storm events or may have long-term effects.

Our results reflect the given model parameters. In the absence of sufficient data for determination of sediment parameters, these were calibrated by comparing the simulated SSC with measured ones or values adopted from literature. The same shortage holds for *F. fabula* abundance data. These were restricted to the locations of observation and were therefore extrapolated and interpolated for other regions. Seasonal variation of macrofauna abundance was not considered. Furthermore, in the present study, the macrofauna effect of a single dominant species was considered ignoring the effect of several other species and their non-linear interaction within the community. The parametrizations adopted for the inclusion of macrofauna effects were based on very limited data from literature. According to Eq. 6, these effects can be highly non-linear, as erodibility increases exponentially between an abundance of 100 to 800 ind. m^{-2}, following a S-shaped equation, leading to highly increased erosion rate in inhabited areas and finally exhausting the available bed material. Another possible limitation of our model is that macrofauna effects were assumed to be constant over time and other macrofauna effects such as those on roughness or biodeposition were not considered. In case of *F. fabula*, however, the temporal variability of abundance is known to be limited (Creutzberg, 1986).

Finally, we suggest more laboratory experiments addressing the functional form of how macrobenthic organisms (communities) alter sediment transport properties. This would greatly reduce the uncertainty in critical model formulations. Also, our results should be verified by field measurements, in which simultaneous measurements of hydrodynamics and sediment concentration as well as bed sediment and biological probes are conducted. This may result in new and more accurate and integral (because biological) parameterizations of sediment transport models.

5 Conclusions

The observed influence of macrofauna on sediments at the seabed and the seabed structure itself has been investigated in terms of large-scale impacts on suspended sediment concentration for a shallow shelf sea. The southern North Sea has been taken as an example to study the impact of macrofauna in a numerical model by integrating a generic benthos module in a coupled 3D model system. Modification of critical bed shear stress and erodibility constituted the major proxies for macrofauna impacts on sediment. What distinguishes the present study from previous ones is the focus on large-scale effects (>100 km) combined with the application of the measured spatial distribution of the bivalve *F. fabula* as a chosen characteristic species.

The simulation results indicate that macrofauna not only can significantly modify SSC locally but also beyond the inhabited zones. As expected, the enhanced SSC due to macrofauna is most pronounced for high energy conditions such as storm events but persists also over a spring-neap tidal cycle. Changes of SSC were not confined near the bed but extended through the water column due to vertical mixing.

Furthermore, it was shown that magnitude and horizontal extent of macrofauna modified SSC are constrained by sediment availability and depend on the sediment properties, such as settling velocity and critical bed shear stress for deposition and erosion. Fine silt, being the dominant fraction for suspended sediment in the water column, was found to be very sensitive to the occurrence of macrofauna. While the present study contributes to the improvement of ecosystem and sediment transport modelling by offering new insights into large-scale effects of macrofauna on SSC in the southern North Sea, it should be noted that physical and biological processes in the model are less complex as in nature and rely partly on simplified parameterizations, which offers various new research questions both in empirical and modeling research.

6 Acknowledgement

This work results from joint efforts of the MOSSCO project partners funded by the German Federal Ministry of Education and Research (BMBF) as part of the Coastal Research Agenda for the North Sea and Baltic Sea (grant numbers 03F0668A, 03F0667A, 03F0667B). We acknowledge the contribution of J. Dannheim and M. Zeiler of the German Federal Maritime and Hydrographic Agency (BSH) by providing us with the *F. fabula* abundance data and Wenyan Zhang from Helmholtz-Zentrum Geesthacht (PACES Programme of the Helmholtz-Gemeinschaft) for completing the data set for the southern North Sea. Processed satellite data have been provided by Brockmann Consult. We acknowledge editing the text by Gregor Melling.

7 Literature

Andersen, T., and M. Pejrup (2011), Biological Influences on Sediment Behavior and Transport, in *Treatise on Estuarine and Coastal Science*, pp. 289–309, Elsevier.

Armanini, A., and G. Di Silvio (1986), A depth-integrated model for suspended sediment transport, *Journal of Hydraulic Research*, *24*(5), 437–442, doi:10.1080/00221688609499319.

Austen, I., T. J. Andersen, and K. Edelvang (1999), The Influence of Benthic Diatoms and Invertebrates on the Erodibility of an Intertidal Mudflat, the Danish Wadden Sea, *Estuarine, Coastal and Shelf Science*, *49*(1), 99–111, doi:10.1006/ecss.1998.0491.

Borsje, B. W., S. Hulscher, M. B. de Vries, and G. J. de Boer (2007), Modeling large scale cohesive sediment transport by including biological activity, *River, Coastal and Estuarine Morphodynamics: RCEM 2007*, 255–262.

Borsje, B. W., Hulscher,Suzanne Jacqueline Marie Hélène, P. M. J. Herman, and M. B. Vries (2009), On the parameterization of biological influences on offshore sand wave dynamics, *Ocean Dynamics*, *59*(5), 659–670, doi:10.1007/s10236-009-0199-0.

Borsje, B. W., M. B. de Vries, S. J. Hulscher, and G. de Boer (2008), Modeling large-scale cohesive sediment transport affected by small-scale biological activity, *Estuarine, Coastal and Shelf Science*, *78*(3), 468–480, doi:10.1016/j.ecss.2008.01.009.

Bremner, J., S. Rogers, and C. Frid (2006), Methods for describing ecological functioning of marine benthic assemblages using biological traits analysis (BTA), *Ecological Indicators*, *6*(3), 609–622, doi:10.1016/j.ecolind.2005.08.026.

Breugem, W. A., and L. H. Holthuijsen (2007), Generalized Shallow Water Wave Growth from Lake George, *J. Waterway, Port, Coastal, Ocean Eng.*, *133*(3), 173–182, doi:10.1061/(ASCE)0733-950X(2007)133:3(173).

Briggs, K. B., G. Cartwright, C. T. Friedrichs, and S. Shivarudruppa (2015), Biogenic effects on cohesive sediment erodibility resulting from recurring seasonal hypoxia on the Louisiana shelf, *Continental Shelf Research*, *93*, 17–26, doi:10.1016/j.csr.2014.11.005.

Burchard, H., and K. Bolding (2002), GETM, A General Estuarine Transport Model: Scientific Documentation, *Technical Report EUR 20253 EN. European Commission*.

Burchard, H., G. Flöser, J. V. Staneva, T. H. Badewien, and R. Riethmüller (2008), Impact of Density Gradients on Net Sediment Transport into the Wadden Sea, *J. Phys. Oceanogr.*, *38*(3), 566–587, doi:10.1175/2007JPO3796.1.

Canuto, V. M., A. Howard, Y. Cheng, and M. S. Dubovikov (2001), Ocean Turbulence. Part I: One-Point Closure Model—Momentum and Heat Vertical Diffusivities, *J. Phys. Oceanogr.*, *31*(6), 1413–1426, doi:10.1175/1520-0485(2001)031<1413:OTPIOP>2.0.CO;2.

Creutzberg, F. (1986), Distribution patterns of two bivalve species (Nucula turgida, Tellina fabula) along a frontal system in the Southern North Sea, *Netherlands Journal of Sea Research*, *20*(2-3), 305–311, doi:10.1016/0077-7579(86)90052-9.

Dannheim, J. (2014), Bewertungsansätze für Raumordnung und Genehmigungsverfahren im Hinblick auf das benthische System und Habitatstrukturen, Statusbericht und Web-Dienst im GeoSeaPortal des BSH: Forschungsvorhaben im Auftrag des BSH.

Darr, A., M. Gogina, and M. L. Zettler (2014), Functional changes in benthic communities along a salinity gradient– a western Baltic case study, *Journal of Sea Research*, *85*, 315–324, doi:10.1016/j.seares.2013.06.003.

Davis, W. R. (1993), The role of bioturbation in sediment resuspension and its interaction with physical shearing, *Journal of Experimental Marine Biology and Ecology*, *171*(2), 187–200, doi:10.1016/0022-0981(93)90003-7.

Deckere, E. de, T. Tolhurst, and J. de Brouwer (2001), Destabilization of Cohesive Intertidal Sediments by Infauna, *Estuarine, Coastal and Shelf Science*, *53*(5), 665–669, doi:10.1006/ecss.2001.0811.

Doerffer, R., H. Schiller, and M. Peters (2006), Meris regional case 2 water algorithms (c2r), www.brockmann-consult.de/beam/software/plugins/merisc2r-1.1.

Duineveld, G., A. Künitzer, U. Niermann, P. de Wilde, and J. S. Gray (1991), The macrobenthos of the north sea, *Netherlands Journal of Sea Research*, *28*(1-2), 53–65, doi:10.1016/0077-7579(91)90004-K.

Duran-Matute, M., T. Gerkema, G. J. de Boer, J. J. Nauw, and U. Gräwe (2014), Residual circulation and freshwater transport in the Dutch Wadden Sea: A numerical modelling study, *Ocean Sci.*, *10*(4), 611–632, doi:10.5194/os-10-611-2014.

François, F., J.-C. Poggiale, J.-P. Durbec, and G. Stora (1997), A New Approach for the Modelling of Sediment Reworking Induced by a Macrobenthic Community, *Acta Biotheoretica*, *45*(3/4), 295–319, doi:10.1023/A:1000636109604.

Gayer, G., S. Dick, A. Pleskachevsky, and W. Rosenthal (2006), Numerical modeling of suspended matter transport in the North Sea, *Ocean Dynamics*, *56*(1), 62–77, doi:10.1007/s10236-006-0070-5.

Graf, G., and R. Rosenberg (1997), Bioresuspension and biodeposition: a review, *Journal of Marine Systems*, *11*(3-4), 269–278, doi:10.1016/S0924-7963(96)00126-1.

Gräwe, U., G. Flöser, T. Gerkema, M. Duran-Matute, T. H. Badewien, E. Schulz, and H. Burchard (2016), A numerical model for the entire Wadden Sea: Skill assessment and analysis of hydrodynamics, *J. Geophys. Res. Oceans*, *121*(7), 5231–5251, doi:10.1002/2016JC011655.

Harris, R. J., C. A. Pilditch, B. L. Greenfield, V. Moon, and I. Kröncke (2016), The Influence of Benthic Macrofauna on the Erodibility of Intertidal Sediments with Varying mud Content in Three New Zealand Estuaries, *Estuaries and Coasts*, *39*(3), 815–828, doi:10.1007/s12237-015-0036-2.

Heath, M. R., A. C. Edwards, J. Patsch, and Turrell Scottish Executive Central Research Unit (2002), Modelling the behaviour of nutrients in the coastal waters of Scotland, nowel, http://strathprints.strath.ac.uk/18568/.

Hetzel, Y., C. Pattiaratchi, R. Lowe, and R. Hofmeister (2015), Wind and tidal mixing controls on stratification and dense water outflows in a large hypersaline bay, *J. Geophys. Res. Oceans*, *120*(9), 6034–6056, doi:10.1002/2015JC010733.

Hill, C., C. DeLuca, Balaji, M. Suarez, and A. Da Silva (2004), The architecture of the earth system modeling framework, *Comput. Sci. Eng.*, *6*(1), 18–28, doi:10.1109/MCISE.2004.1255817.

Hofmeister, R., K. Bolding, R. D. Hetland, G. Schernewski, H. Siegel, and H. Burchard (2013), The dynamics of cooling water discharge in a shallow, non-tidal embayment, *Continental Shelf Research*, *71*, 68–77, doi:10.1016/j.csr.2013.10.006.

Hofmeister, R., H. Burchard, and J.-M. Beckers (2010), Non-uniform adaptive vertical grids for 3D numerical ocean models, *Ocean Modelling*, *33*(1-2), 70–86, doi:10.1016/j.ocemod.2009.12.003.

Hofmeister, R., C. Lemmen, O. Kerimoglu, K. W. Wirtz, and M. H. Nasermoaddeli (2014), The predominant processes controlling vertical nutrient and suspended matter fluxes across domains - using the new MOSSCO system form coastal sea sediments up to the atmosphere, in *ICHE-2014 11th International Conference on Hydroscience and Engineering: Hydro-Engineering for Environmental Challenges*, edited by Lehfeldt, R., Kopmann , R., Hydro-Engineering for Environmental Challenges.

Jumars, P. A., and A. Nowell (1984), Effects of benthos on sediment transport: difficulties with functional grouping, *Continental Shelf Research*, *3*(2), 115–130, doi:10.1016/0278-4343(84)90002-5.

Kappenberg, J., and I. Grabemann (2001), Variability of the Mixing Zones and Estuarine Turbidity Maxima in the Elbe and Weser Estuaries, *Estuaries*, *24*(5), 699, doi:10.2307/1352878.

Kerimoglu, O., R. Hofmeister, J. Maerz, and K. Wirtz (in prep.), A novel adaptive biogeochemical model and its 3D application for a decadal hindcast simulation of the biogeochemistry of the southern North Sea.

Klingbeil, K., and H. Burchard (2013), Implementation of a direct nonhydrostatic pressure gradient discretisation into a layered ocean model, *Ocean Modelling*, *65*, 64–77, doi:10.1016/j.ocemod.2013.02.002.

Klingbeil, K., M. Mohammadi-Aragh, U. Gräwe, and H. Burchard (2014), Quantification of spurious dissipation and mixing – Discrete variance decay in a Finite-Volume framework, *Ocean Modelling*, *81*, 49–64, doi:10.1016/j.ocemod.2014.06.001.

Knaapen, M., H. Holzhauer, S. Hulscher, M. J. Baptist, M. d. Vries, and M. van Ledden (2003), On the modelling of biological effects on morphology in estuaries and seas, edited by A. Sánchez-Arcilla and A. Bateman, pp. 773–783, IHAR.

Krause, G., G. Budeus, D. Gerdes, K. Schaumann, K. Hesse (1986), Frontal systems in the German Bight and their physical and biological effects, in: Nihoul, J.C.J. (Ed.) Marine interfaces ecohydrodynamics: proceedings of the 17th International Liège Colloquium on Ocean Hydrodynamics. Elsevier Oceanography Series, 42, 119-140

Kristensen, E., J. M. Neto, M. Lundkvist, L. Frederiksen, M. Â. Pardal, T. Valdemarsen, and M. R. Flindt (2013), Influence of benthic macroinvertebrates on the erodability of estuarine cohesive sediments: Density- and biomass-specific responses, *Estuarine, Coastal and Shelf Science*, doi:10.1016/j.ecss.2013.09.020.

Kröncke, I., H. Reiss, J. D. Eggleton, J. Aldridge, M. J. Bergman, S. Cochrane, J. A. Craeymeersch, S. Degraer, N. Desroy, J.-M. Dewarumez, G. C. Duineveld, K. Essink, H. Hillewaert, M. S. Lavaleye, A. Moll, S. Nehring, R. Newell, E. Oug, T. Pohlmann, E. Rachor, M. Robertson, H. Rumohr, M. Schratzberger, R. Smith, E. V. Berghe, J. van Dalfsen, G. van Hoey, M. Vincx, W. Willems, and H. L. Rees (2011), Changes in North Sea macrofauna communities and species distribution between 1986 and 2000, *Estuarine, Coastal and Shelf Science*, *94*(1), 1–15, doi:10.1016/j.ecss.2011.04.008.

Krumbein, W. E. (1994), *Biostabilization of sediments*, 526 pp., Carl-von-Ossietzky-Univ. Oldenburg, Oldenburg.

Le Hir, P., Y. Monbet, and F. Orvain (2007), Sediment erodability in sediment transport modelling: Can we account for biota effects?, *Continental Shelf Research*, *27*(8), 1116–1142, doi:10.1016/j.csr.2005.11.016.

Lemmen, C., H. Burchard, R. Hofmeister, O. Kerimoglu, K. Klingbeil, F. Kösters, M. H. Nasermoaddeli, and K. W. Wirtz (2017), Modular System for Shelves and Coasts (MOSSCO), *Geosci. Model Dev.*(to be subm.).

Lemmen, C., R. Hofmeister, and K. W. Wirtz (2013), Das Modulare System für Schelfmeer und Küsten (MOSSCO) - Konzepte und Infrasturktur zum Zusammenwirken verschiedener Modelle für die Küstenforschung.

Lettmann, K. A., J.-O. Wolff, and T. H. Badewien (2009), Modeling the impact of wind and waves on suspended particulate matter fluxes in the East Frisian Wadden Sea (southern North Sea), *Ocean Dynamics*, *59*(2), 239–262, doi:10.1007/s10236-009-0194-5.

Lumborg, U., T. J. Andersen, and M. Pejrup (2006), The effect of *Hydrobia ulvae* and microphytobenthos on cohesive sediment dynamics on an intertidal mudflat described by means of numerical modelling, *Estuarine, Coastal and Shelf Science*, *68*(1–2), 208–220, doi:10.1016/j.ecss.2005.11.039.

Maa, J. P.-Y., J.-I. Kwon, K.-N. Hwang, and H.-K. Ha (2008), Critical Bed-Shear Stress for Cohesive Sediment Deposition under Steady Flows, *J. Hydraul. Eng.*, *134*(12), 1767–1771, doi:10.1061/(ASCE)0733-9429(2008)134:12(1767).

Mohammadi-Aragh, M., K. Klingbeil, N. Brüggemann, C. Eden, and H. Burchard (2015), The impact of advection schemes on restratifiction due to lateral shear and baroclinic instabilities, *Ocean Modelling*, *94*, 112–127, doi:10.1016/j.ocemod.2015.07.021.

Montague, C. L. (1986), Influence of Biota on Erodibility of Sediments, in *Estuarine cohesive sediment dynamics: Proceedings of a workshop on cohesive sediment dynamics with special reference to physical processes in estuaries, Tampa, Florida, November 12-14, 1984*, *Lecture Notes on Coastal and Estuarine Studies*, vol. 14, edited by A. J. Mehta, pp. 251–269, Springer-Verlag, Berlin, New York.

Montserrat Trotsenburg, F. (2011), Estuarine ecosystem engineering: biogeomorphology in the estuarine intertidal, Dissertation, Civil Engineering and Geosciences, Hydraulic Engineering, Technische Universiteit Delft, Delft.

Nasermoaddeli, M. H., C. Lemmen, R. Hofmeister, F. Koesters, and K. Klingbeil (2014), The benthic geoecology model within the modular system for shelves and coasts (MOSSCO), in *HIC2014-11. International Conference on Hydroinformatics: Informatics and the Environment: Data and Model Integration in a Heterogeneous Hydro World*, edited by M. Piaseki, City University of New York, New York, USA.

Neumann, H., H. Reiss, S. Ehrich, A. Sell, K. Panten, M. Kloppmann, I. Wilhelms, and I. Kröncke (2012), Benthos and demersal fish habitats in the German Exclusive Economic Zone (EEZ) of the North Sea, *Helgol Mar Res*, doi:10.1007/s10152-012-0334-z.

Nowell, A. R. M., and P. A. Jumars (1984), Flow environments of aquatic benthos, *Annual Review of Ecology and Systematics*, *15*, 303–328.

Orvain, F. (2005), A model of sediment transport under the influence of surface bioturbation: generalisation to the facultative suspension-feeder Scrobicularia plana, *Mar. Ecol. Prog. Ser.*, *286*, 43–56, doi:10.3354/meps286043.

Orvain, F., K. Guizien, S. Lefebvre, M. Bréret, and C. Dupuy (2014), Relevance of macrozoobenthic grazers to understand the dynamic behaviour of sediment erodibility and microphytobenthos resuspension in sunny summer conditions, *Journal of Sea Research*, doi:10.1016/j.seares.2014.03.004.

Orvain, F., P. Le Hir, and P.-G. Sauriau (2003), A model of fluff layer erosion and subsequent bed erosion in the presence of the bioturbator, *Hydrobia ulvae*, *J Mar Res*, *61*(6), 821–849, doi:10.1357/002224003322981165.

Orvain, F., P. Le Hir, P.-G. Sauriau, and S. Lefebvre (2012), Modelling the effects of macrofauna on sediment transport and bed elevation: Application over a cross-shore mudflat profile and model validation, *Estuarine, Coastal and Shelf Science*, *108*, 64–75, doi:10.1016/j.ecss.2011.12.036.

Orvain, F., P.-G. Sauriau, C. Bacher, and M. Prineau (2006), The influence of sediment cohesiveness on bioturbation effects due to Hydrobia ulvae on the initial erosion of intertidal sediments: A study combining flume and model approaches, *Journal of Sea Research*, *55*(1), 54–73, doi:10.1016/j.seares.2005.10.002.

Paarlberg, A. J., M. Knaapen, M. B. de Vries, S. Hulscher, and Z. B. Wang (2005), Biological influences on morphology and bed composition of an intertidal flat, *Estuarine, Coastal and Shelf Science*, *64*(4), 577–590, doi:10.1016/j.ecss.2005.04.008.

Partheniades, E. (1965), Erosion and Deposition of Cohesive Soils, *Journal of the Hydraulics Division*, *91*(1), 105–139.

Paterson, D. M. and Black, K. S. (1999), Water flow, sediment dynamics and benthic biology, *Advances in Ecological Research*, *29*, 155–193.

Peine, F., B. Bobertz, and G. Graf (2005), Influence of the blue mussel *Mytilus edulis* (Linnaeus) on the bottom roughness length (z_0) in the south-western Baltic Sea, *Baltica*, *18*(1), 13–22.

Pleskachevsky, A., G. Gayer, J. Horstmann, and W. Rosenthal (2005), Synergy of satellite remote sensing and numerical modeling for monitoring of suspended particulate matter, *Ocean Dynamics*, *55*(1), 2–9, doi:10.1007/s10236-004-0101-z.

Postma, H. (1984), Introduction to the symposium on organic matter in the Wadden Sea, *Neth. Inst. Sea Res. Pub. Ser.*, *10*, 15–22.

Puls, W., J. Beusekom, U. Brockmann, R. Doerffer, U. Hentschke, P. König, D. Murphy, B. Mayer, A. Müller, T. Pohlmann, A. Reimer, R. Schmidt-Nia, and J. Sündermann (1999), SPM concentrations in the German Bight: Comparison between a model simulation and measurements, *Deutsche Hydrographische Zeitschrift*, *51*(2-3), 221–244, doi:10.1007/BF02764175.

Puls, W., H. Kühl, A. Frohse, and P. König (1995), Measurements of the suspended matter settling velocity in the German Bight (North Sea), *Deutsche Hydrographische Zeitschrift*, *47*(4), 259–276, doi:10.1007/BF02737787.

Puls, W., T. Pohlmann, and J. Sündermann (1997), Suspended particulate matter in the Southern North Sea: Application of a numerical model to extend NERC North Sea project data interpretation, *Deutsche Hydrographische Zeitschrift*, *49*(2-3), 307–327, doi:10.1007/BF02764041.

Purkiani, K., J. Becherer, K. Klingbeil, and H. Burchard (2016), Wind-induced variability of estuarine circulation in a tidally energetic inlet with curvature, *J. Geophys. Res. Oceans*, *121*(5), 3261–3277, doi:10.1002/2015JC010945.

Rachor, E., and P. Nehmer (2003), Erfassung und Bewertung ökologisch wertvoller Lebensräume in der Nordsee, 175 pp., Bundesamt für Naturschutz, Bremerhaven, hdl:10013/epic.36744.d001.

Radach, G., and J. Pätsch (2007), Variability of continental riverine freshwater and nutrient inputs into the North Sea for the years 1977–2000 and its consequences for the assessment of eutrophication, *Estuaries and Coasts*, *30*(1), 66–81, doi:10.1007/BF02782968.

Reiss, H., S. Cunze, K. König, H. Neumann, and I. Kröncke (2011), Species distribution modelling of marine benthos: a North Sea case study, *Mar. Ecol. Prog. Ser.*, *442*, 71–86, doi:10.3354/meps09391.

Rhoads, D. C., J. Y. Yingst, and W. J. Ullmann (1978), Sea floor stability in Long Island Sound. Part I. Temporal changes in erodibility of fine grained sediments, in *Estuarine Interactions*, edited by M.L. Wiley, Academic Press, New York, USA.

Rijkswaterstaat (2017), Waterbase, http://live.waterbase.nl/ [accessed 19 Jan 2017].

Salzwedel, H., E. Rachor, and D. Gerdes (1985), Benthic macrofauna communities in the German Bight, *Veröff. Inst. Meeresforsch. Bremerh.*, *20*, 199–267.

Sanford, L. P. (2008), Modeling a dynamically varying mixed sediment bed with erosion, deposition, bioturbation, consolidation, and armoring, *Computers & Geosciences*, *34*(10), 1263–1283, doi:10.1016/j.cageo.2008.02.011.

Schrum, C. (1997), Thermohaline stratification and instabilities at tidal mixing fronts: Results of an eddy resolving model for the German Bight, *Continental Shelf Research*, *17*(6), 689–716, doi:10.1016/S0278-4343(96)00051-9.

Seifert, T., W. Fennel, and C. Kuhrts (2009), High resolution model studies of transport of sedimentary material in the south-western Baltic, *Journal of Marine Systems*, *75*(3-4), 382–396, doi:10.1016/j.jmarsys.2007.01.017.

Shimeta, J., C. L. Amos, S. E. Beaulieu, and O. M. Ashiru (2002), Sequential resuspensionof protists by accelerating tidal flow: implications for community structure in the benthic boundary layer, *Limnol. Oceangr.*, *47*, 1152–1164.

Smagorinsky, J. (1963), General circulation experiments with the primitive equations, *Mon. Wea. Rev.*, *91*(3), 99–164, doi:10.1175/1520-0493(1963)091<0099:GCEWTP>2.3.CO;2.

Soulsby, R. (1997), *Dynamics of marine sands: A manual for practical applications*, 1st ed., Telford, London.

Stammermann, R., and M. Piasecki (2012), Influence of Sediment Availability, Vegetation, and Sea Level Rise on the Development of Tidal Marshes in the Delaware Bay: A Review, *Journal of Coastal Research*, *285*, 1536–1549, doi:10.2112/JCOASTRES-D-11-00143.1.

Stanev, E. V., R. Al-Nadhairi, J. Staneva, J. Schulz-Stellenfleth, and A. Valle-Levinson (2014), Tidal wave transformations in the German Bight, *Ocean Dynamics*, *64*(7), 951–968, doi:10.1007/s10236-014-0733-6.

Stanev, E. V., M. Dobrynin, A. Pleskachevsky, S. Grayek, and H. Günther (2009), Bed shear stress in the southern North Sea as an important driver for suspended sediment dynamics, *Ocean Dynamics*, *59*(2), 183–194, doi:10.1007/s10236-008-0171-4.

Stips, A., K. Bolding, T. Pohlmann, and H. Burchard (2004), Simulating the temporal and spatial dynamics of the North Sea using the new model GETM (general estuarine transport model), *Ocean Dynamics*, *54*(2), 266–283, doi:10.1007/s10236-003-0077-0.

Umlauf, L., and H. Burchard (2005), Second-order turbulence closure models for geophysical boundary layers. A review of recent work, *Continental Shelf Research*, *25*(7-8), 795–827, doi:10.1016/j.csr.2004.08.004.

van der Molen, J., K. Bolding, N. Greenwood, and D. K. Mills (2009), A 1-D vertical multiple grain size model of suspended particulate matter in combined currents and waves in shelf seas, *J. Geophys. Res.*, *114*(F1), doi:10.1029/2008JF001150.

van Hulten, M. M. P., A. Sterl, R. Middag, H. J. W. de Baar, M. Gehlen, J.-C. Dutay, and A. Tagliabue (2014), On the effects of circulation, sediment resuspension and biological incorporation by diatoms in an ocean model of aluminium*, *Biogeosciences*, *11*(14), 3757–3779, doi:10.5194/bg-11-3757-2014.

van Ledden, M. (2003), *Sand-mud segregation in estuaries and tidal basins*, xvi, 218, *Communications on hydraulic and geotechnical engineering*, report no. 03-2, Dept. of Civil Engineering and Geosciences, Delft University of Technology, Delft.

van Ledden, M., W. van Kesteren, and J. Winterwerp (2004), A conceptual framework for the erosion behaviour of sand–mud mixtures, *Continental Shelf Research*, *24*(1), 1–11, doi:10.1016/j.csr.2003.09.002.

van Leeuwen, S. M., J. van der Molen, P. Ruardij, L. Fernand, and T. Jickells (2013), Modelling the contribution of deep chlorophyll maxima to annual primary production in the North Sea, *Biogeochemistry*, *113*(1-3), 137–152, doi:10.1007/s10533-012-9704-5.

van Moorsel, G. (2011), Species and habitats of the international Dogger Bank, ecosub, Doorn. 74 p.

van Prooijen, Bram C., F. Montserrat, and P. M. Herman (2011), A process-based model for erosion of Macoma balthica-affected mud beds, *Continental Shelf Research*, *31*(6), 527–538, doi:10.1016/j.csr.2010.12.008.

Wheatcroft, R. A., and C. A. Butman (1997), Spatial and temporal variability in aggregated grain-size distributions, with implications for sediment dynamics, *Continental Shelf Research*, *17*(4), 367–390, doi:10.1016/S0278-4343(96)00035-0.

Widdows, J., M. Brinsley, and M. Elliott (1998), Use of in situ flume to quantify particle flux (biodeposition rates and sediment erosion) for an intertidal mudflat in relation to changes in current velocity and benthic macrofauna, *Geological Society, London, Special Publications*, *139*(1), 85–97, doi:10.1144/GSL.SP.1998.139.01.07.

Widdows, J., M. Brinsley, P. N. Salkeld, and C. H. Lucas (2000a), Influence of biota on spatial and temporal variation in sediment erodability and material flux on a tidal flat (Westerschelde, The Netherlands), *Marine Ecology Progress Series*, *194*, 23–37.

Widdows, J., S. Brown, M. Brinsley, P. Salkeld, and M. Elliott (2000b), Temporal changes in intertidal sediment erodability: influence of biological and climatic factors, *Continental Shelf Research*, *20*(10-11), 1275–1289, doi:10.1016/S0278-4343(00)00023-6.

Winterwerp, J. C. (2007), On the sedimentation rate of cohesive sediment, in *Estuarine and Coastal Fine Sediments Dynamics - Intercoh 2003*, *Proceedings in Marine Science*, pp. 209–226, Elsevier.

Winterwerp, J. C., and W. G. M. van Kesteren (2004), *Introduction to the physics of cohesive sediment in the marine environment*, 1st ed., 1 online resource (1 volume (various, *Developments in sedimentology*, vol. 56, Elsevier, Amsterdam.

Wood, R., and J. Widdows (2002), A model of sediment transport over an intertidal transect, comparing the influences of biological and physical factors, *Limnol. Oceangr.*, *47*(3), 848–855, doi:10.4319/lo.2002.47.3.0848.